Effect of Magnetic Materials on the In-Vessel Magnetic Configuration in KSTAR

S. W. Yoon, A. C. England, W. C. Kim, H. Yonekawa, J. G. Bak, Y. K. Oh, B. H. Park, J. Kim, K. I. You, Y. M. Jeon, S. H. Hahn, Y. K. Oh, J. Chung, K.D. Lee, H .J. Lee[1]
J. A. Leuer[2], N. W. Eidietis[2]

[1]*National Fusion Research Institute, 113 Gwahangno, Yusung-Gu, Daejeon, 305-333, Korea*
[2]*General Atomics, 3550 General Atomics Court, San Diego, CA 92121, USA*

I. INTRODUCTION

It was observed in KSTAR during the first campaign that there was a significant discrepancy between the measured and the calculated poloidal vacuum magnetic fields (B). This was mainly due to the presence of an inherent magnetic material used for the conduit of the superconducting strands. The material is called Incoloy 908 [1] and it was originally chosen for ITER based on its excellent thermo-mechanical properties. However, it is weakly ferromagnetic and its relative magnetic permeability (μ_r) is around 10 at 4.5 K and at low B it shows a small amount of hysteresis. The effect of Incoloy on KSTAR plasmas is not fully understood yet but its impact on plasma initiation is significant judging from the in-situ measurements of the vacuum magnetic field. It was reported also in the last two campaigns that the operation boundary of the startup process in KSTAR was narrow both in pre-fill neutral pressure and field-null size and hence the discharge reproducibility was poor. This might be partially attributable to the additional field from Incoloy. In addition, with symmetric up-down charging of all poloidal field (PF) coils, the vertical position of the plasma current (Zp) was about 10 cm below the midplane suggesting the existence of a radial field, Br, at the midplane during the plasma flattop.

In this work, the effect of Incoloy 908 on the field-null configuration during the startup phase in KSTAR was studied using extensive measurements of the field-null structure and model nonlinear calculations of the perturbed field from Incoloy. In addition, the potential sources of the midplane Br were analyzed focusing on the up-down asymmetric eddy currents in the cryostat structure. In section II, the diagnostic setup of the magnetic field measurement systems is described including the usual pick-up coils and flux loops, Hall sensor (HS) arrays near the field-null center, and an electron beam (E-beam) probe. In section III, the data analysis and drift correction method is presented and the calculation models are briefly explained including the typical circuit equations and the nonlinear Finite Element Method (FEM) calculations for Incoloy 908. The comparison between the measured and the calculated fields is presented and the saturation effect is analyzed in section IV. The impact of the perturbative field from Incoloy 908 on the initial current ramp-up is discussed in terms of radial positional stability and the relevant field index criteria. Finally, the effect of eddy currents in the cryostat on Zp are addressed based on the reconstructed eddy currents.

II. DIAGNOSTICS SETUP

To analyze the perturbative fields from Incoloy 908, several independent measurement techniques were employed for cross-check and measurement validation. Besides the routine arrays of pick-up B-probes around the vacuum vessel, the radial and vertical profiles of magnetic field near the field-null region were directly measured with two separate movable insertion systems of Hall sensor (HS) arrays. In addition, the remnant field and the coil

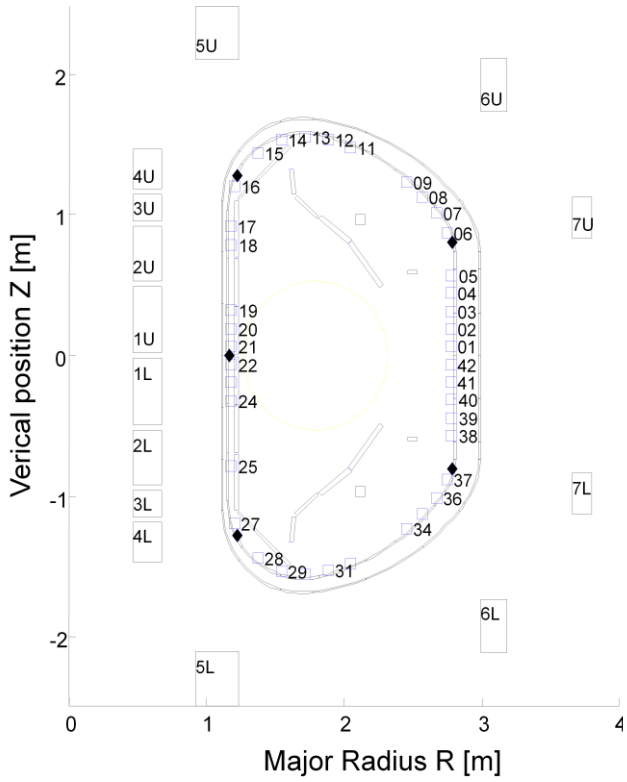

Fig. 1. The positions of magnetic probes. Squares are the position of probes and directions are shown with arrows. The filled diamonds are the positions of the five flux loops. The index of probes starts from the outer midplane and increases counterclockwise. The labels of flux loop are 01, 12, 23, 34 and 45 counterclockwise starting from outer upper midplane.

misalignment errors were assessed with an E-beam probe which measured the toroidally averaged B in contrast to the local ΔB measurement of the pick-up probes [2].

In fig. 1, the positions of the pick-up probes in the poloidal array are shown. At each position, a radial and a vertical probe is installed for a complete coverage of the vacuum vessel boundary in the poloidal direction. However, due to the drift of the integrators, a linear correction was applied numerically and the result was that the correction is reliable at least up to tens of seconds and the errors from the drift are reduced to less than 1% of the nominal value.

An electron beam (E-beam) probe system was inserted at one of the vertical upper ports, which was designed to cover Z=-11 cm to Z=11 cm near the midplane for measurements of up-down asymmetry. The system measured the toroidally integrated perpendicular field along the electron beam path using a scintillator coated screen and a CCD camera. The locations of the returning electron beam spots on the screen along the toroidal direction were measured. The position difference between the starting and return spots is proportional to the ratio of perpendicular and toroidal field B_p/B_T. However, due to the limitation of the access inside vessel, the radial position of the E-beam system was fixed at R=2.02 m and not at the usual major radius of the plasma, R = 1.8 m. Therefore, field-null measurements were done with an R=2.02 m field-null scenario instead. The main advantage of the E-beam system is that it measures a total toroidally averaged B rather than a local delta B which is typical for pickup probes and Hall sensors due to the integrator the orientation issues. Therefore, it is ideal for axisymmetric error field measurements from TF and PF coils.

Finally, an array of Hall sensors was attached to the upper part of the E-beam system. It consisted of 5 sets of detectors 10 cm apart with each set being comprised of a vertical and a radial sensor. In addition to the vertical system, an independent radial probe insertion system was provided from the outer midplane. It was comprised of 2 sets of detectors 15 cm apart for full coverage of the radial and vertical profiles.

There are some weak and strong points of each measurement system. Hall sensors and an E-beam are ideal for direct field-null measurement for initial PF charging state. However, they are not suitable for the dynamic measurements during initial Ip ramp-up due to the eddy currents in the metal sensor case and a required long CCD exposure time~0.5s. In contrast, the pick-up probes are ideal for eddy current measurements during the initial Ip ramp-up phase.

III. CALCULATION MODELS

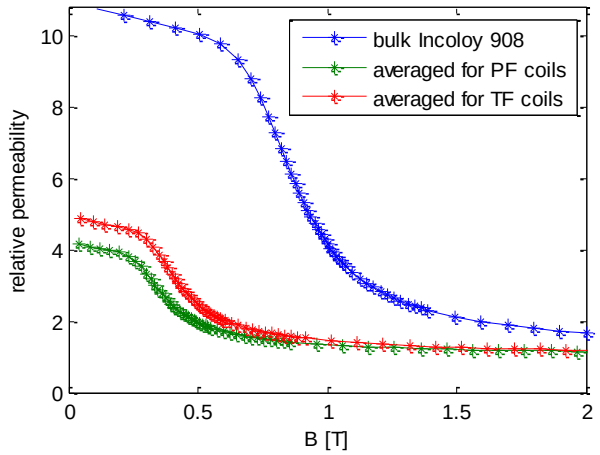

Fig 2. The nonlinear dependence of relative permeability measured by PPMS.

To estimate the perturbative field from Incoloy 908, a FEM model was developed using the nonlinear B-H characteristics of Incoloy. The relative permeability $\mu_r(B)$ was measured for a slice of Incoloy 908 using a physical property measurement system (PPMS) at cryogenic temperature ~4K and is shown fig. 2, neglecting a small remnant field. The magnetization of bulk Incoloy, which saturates around B=1 T, it is required to model the full non-linear range for the KSTAR operation. To reduce the model complexity, each PF coil was simplified as a single turn element rather than the many actual windings. The volume fractions of Incoloy in the coils are 32% for PF and 40% for TF coils. Using the relative fraction of Incoloy in the coils, the effective μ_r's were derived averaging the magnetization inside the coil cross-section (fig. 1). The **Incoloy** was used as the conduit only for the Nb_3Sn strands and the Incoloy in the PF coils was modeled in an averaged manner. In addition, in a 2-D model, the Incoloy in the TF coils was assumed to be saturated in the toroidal direction at high B_{TF} and was neglected for the simple 2-D model. The saturation field for Incoloy is around 1 T and the result was that for a TF coil charging current of more than 15 kA, the Incoloy in the TF coils was close to full saturation and its effect on the poloidal field was negligible. Therefore, ignoring Incoloy from TF coils, a simpler two dimensional model was considered including a toroidally symmetric contribution only from the PF Incoloy which was generally not saturated during the typical PF coil operation. Based on the 2-D FEM Incoloy model, a FEM reconstruction tool was also developed for the eddy current distribution in the vessel as well as determination of Ip, Zp and the plasma current radial position, Rp, using the array of pick-up probes. The plasma cross-section was assumed to be circular, the nonlinear effect from Incoloy was considered self-consistently, and the real shapes of the vessel elements were included, which was numerically effective in the reconstruction of eddy currents with a small number of vessel elements.

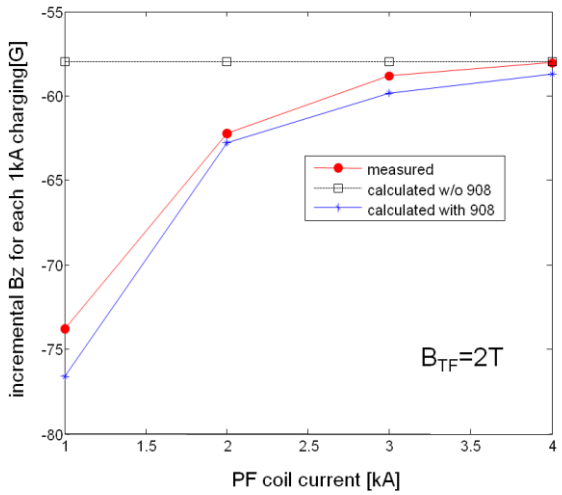

Fig 3. The comparison between the measurements and the calculations at R=2.02 m. The field generated per 1 kA of PF1 charging is shown for different levels of PF1 charging. It is clearly shown that the magnetization in the PF1 coils is saturated at I_{PF}=4 kA. B_{TF}=2 T.

Besides the static FEM model, a time-dependent model of eddy currents in the conducting structure was developed. In this case, the current densities of the PF coil currents were given as the input parameters and the induced electric field was calculated which was directly compared with the measured loop voltage. In addition, the model predicted the eddy current

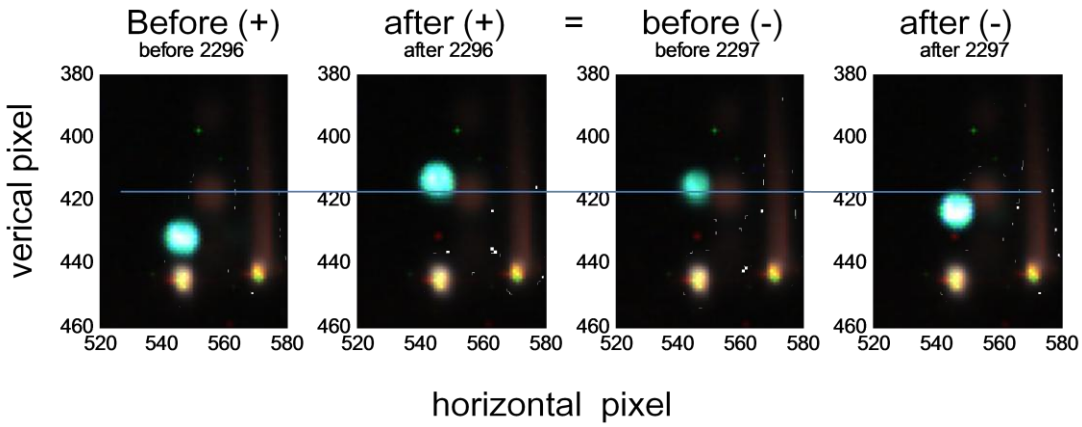

Fig 4. Measurements of the remnant field by the E-beam system at R=2.02 m on the midplane. The blue spots are the first pass e-beam before and after PF charging. Before shot 2296, due to the charging of a single coil, there is about 15 G of Brem. However, by the field-null charging, Brem is reduced to ~3 G max and the effect of the charging history is negligible. One pixel corresponds to 1 G in the figure.

distribution in the conducting structure including the vacuum vessel and the cryostat, which was directly compared to the Rogowski coil measurements.

In fig. 3, the nonlinear μ_r and its saturation effect were validated with a single coil charging test. First of all, the calculated and measured values were in good agreement within a few gauss when the average model of Inconel was applied. Here, it was shown that at low I_{PF}, the field generation per 1 kA of charging deviated from the calculated value without Incoloy. However, as I_{PF} increased, the measured field approached the calculated field and the measured saturation of the PF Incoloy was well described by the model calculations.

IV. EFFECT OF INCOLOY IN THE PF COILS

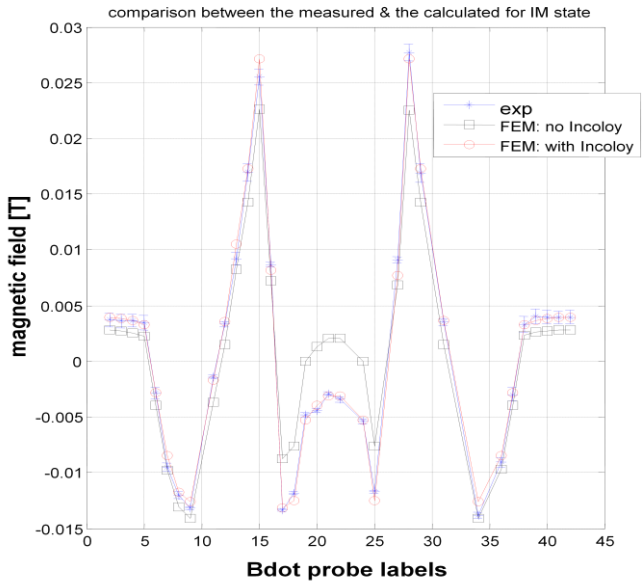

Fig 5. Comparison between the field measured by pickup probes and the field calculated by the FEM model for the initial field-null charging (shot 20 68). The labels start from the outboard midplane counterclockwise. The inboard midplane is between 22 and 23. B_{TF}=2 T.

Firstly, the existence of the remnant field, Brem, was measured with the E-beam system (fig 4). Before shot 2296, a positive charging of the outer PF 7 coil resulted in more than 10 G of Brem and this was due to the alignment of all magnetizations in the central solenoid stack. However, when field-null charging of all PF coils was applied, Brem was reduced to less than 3 G and was rather symmetric with both positive and negative charging. Therefore it is expected that that Brem is 3 G max and no significant effect from the previous charging history existed for the startup experiment.

In fig 5, for the initial field-null configuration, the measured field from the pickup probes is compared with the calculated field with the 2-D nonlinear FEM model with PF

Incoloy only. Generally, the calculated field is in good agreement the measured field only when the PF Incoloy is included in the model. The effect of Incoloy is stronger near the inboard side and the additional field from Incoloy is more than 50 G as shown in the figure.

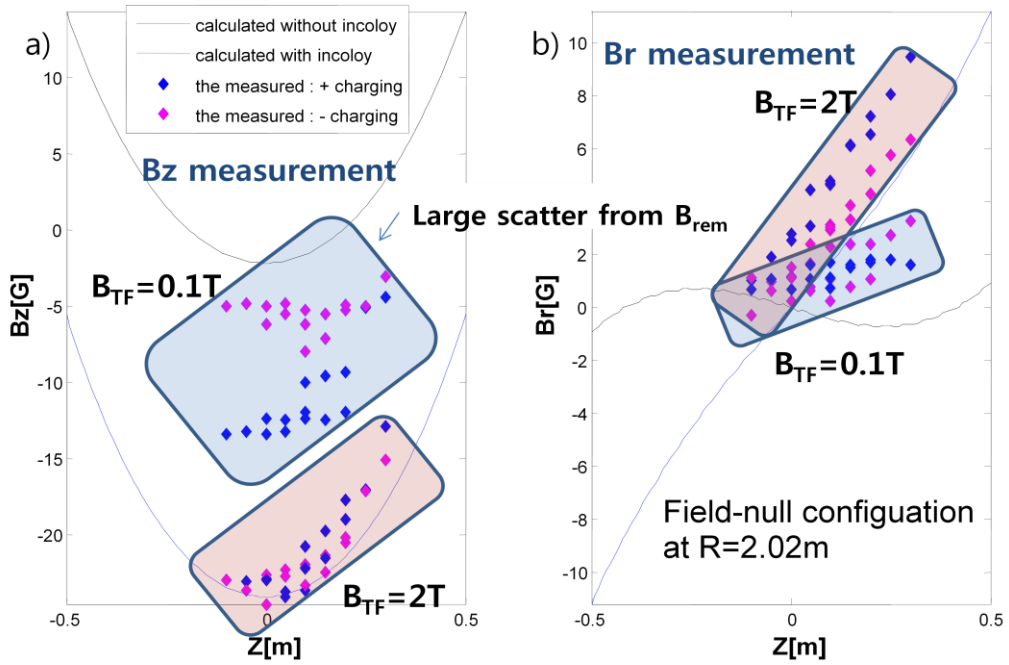

Fig 6. Comparison of the (a) measured and the calculated (FEM) Bz and (b) measured and the calculated (FEM) Br for the field-null state. Results are shown for low toroidal field (0.1 T) where the Incoloy is not saturated and high toroidal field (2 T) where most of the Incoloy is saturated. The FEM calculations assume the Incoloy is saturated and should be compared with the pink region. The effect of Incoloy in the TF coils was not included in the FEM models.

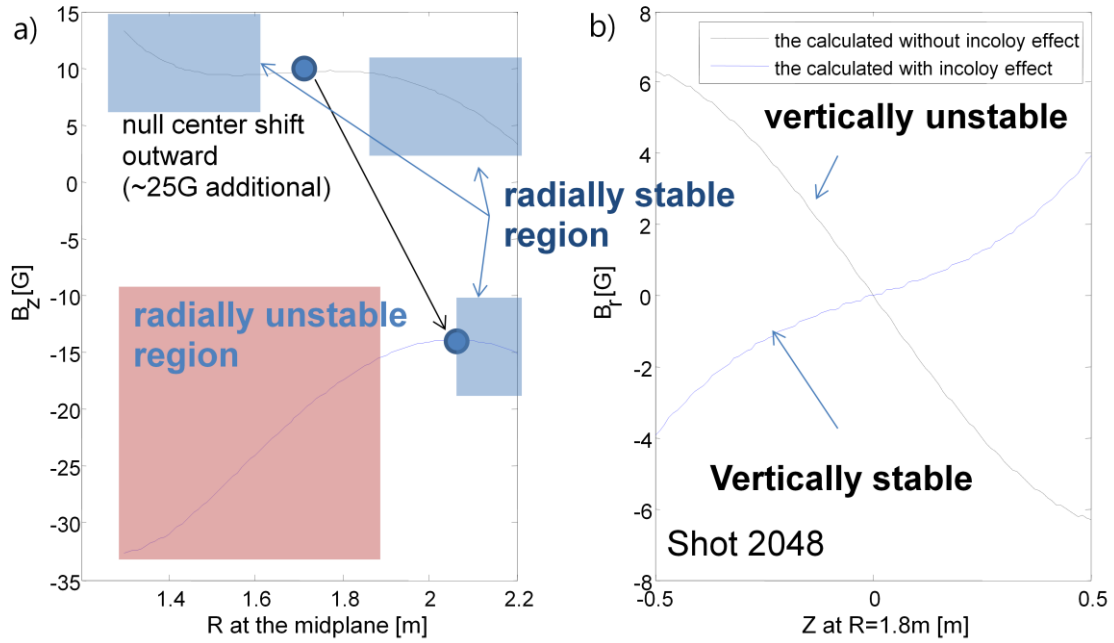

Fig. 7. The effect of Incoloy on the field-null. The sign of B_z & B_r near the field-null center changed due to the influence of Incoloy.

The initial comparison between the measured and the calculated field is shown in fig. 6 for direct measurements for field-null quality with the Hall sensor array. At low B_{TF} (0.1 T), the

discrepancy between (+) and (-) PF coil charging is large due to the presence of the remnant field which is found to be more than 10 G at low B_{TF}. However, as the B_{TF} increased to 2 T,

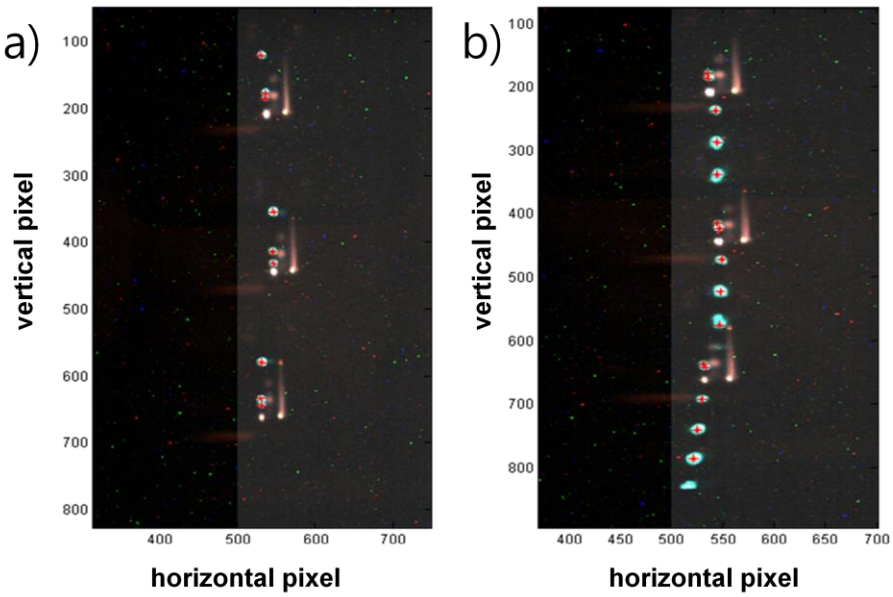

Fig. 8. The CCD images overlaid for the positions of Z=-11, 0, 11 cm of the E-beam probe at the initial magnetic state for field-null at R=2.02 m. a) positive charging of PF coils. b) negative charging of PF coils

the remnant field became small and both measurements matched relatively well with the 2-D non-linear PF Incoloy model for the B_z profiles near the field-null region. This suggests that the major source of the remnant field at low B_{TF} is Incoloy in the TF coils and not in the PF coils. The match is slightly worse for the B_r profiles partly due to orientational accuracy limitations of the HS system and partly to the remnant field. However, the profile itself is very similar to the calculated profile except for a small offset. Roughly speaking, the Incoloy generated approximately -20 G of vertical field at the field-null center and its inclusion in the startup scenario development was important to the overall startup success.

Based on the FEM analysis of Incoloy, it was determined that the effect of Incoloy on the startup was not trivial. Although the effect of Incoloy on the vertical field profile is roughly constant and it does not significantly change the vertical profile, its effect on the radial profile is more complicated. As shown in fig. 7, due to a strong effect from the Incoloy in the central solenoid, the radial profile is completely different from the case without Incoloy. Consequently, not only did it degrade the initial field-null quality but the positional stability of the initial plasma column could be affected by the modified field index [3] from Incoloy and therefore a simple offset correction for Incoloy is only partially effective. This initial configuration occurs 30 ms earlier than breakdown and the field pattern at 30 ms later will be uncertain due to the eddy currents in the vessel. However, the initial charging state illustrates the essential effect of Incoloy on the startup.

V. UP-DOWN ASYMMETRY AND EDDY CURRENTS IN CRYOSTAT

The downshift of plasma column during the ramp-up phase suggested the existence of a certain level of radial magnetic field (Br) at the midplane and the potential sources of Br were investigated. Firstly, the up-down asymmetry of the static field configuration was examined for the initial charging state. By adjusting the position of the E-beam probe vertically, the vertical Br profile near field-null center was measured.

As shown in fig. 8, though there is more than 10 G of Bz, the level of Br is very small and is less than 1 G which is close to the measurement limit, i.e., 1 pixel of the CCD image is 1 G

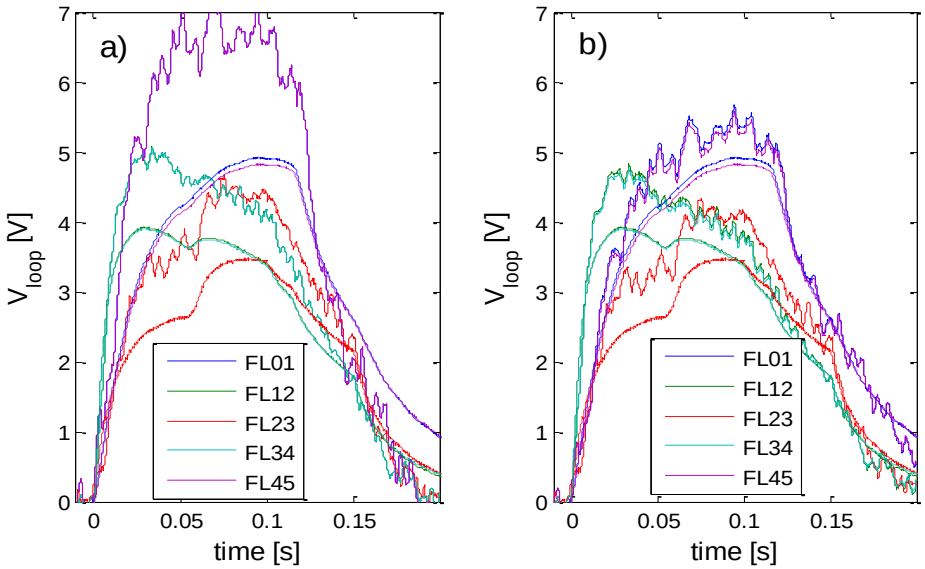

Fig. 9. The comparison of the simulated loop voltages with the measured. a) without cryostat b) with cryostat. For a vacuum discharge (shot 2068).

for B_{TF}=1 T. In addition, using the multi-pass E-beam spots for different positions of the E-beam probe, which is clear for the negative PF charging (fig. 8b), the vertical profiles of Br near the midplane were approximately flat and there was no significant up-down asymmetry in the measured Br profiles. Therefore, coil misalignment error fields do not explain the downshift of plasma. A Br value of less than 1 G cannot cause the observed 10 cm downshift of the plasma.

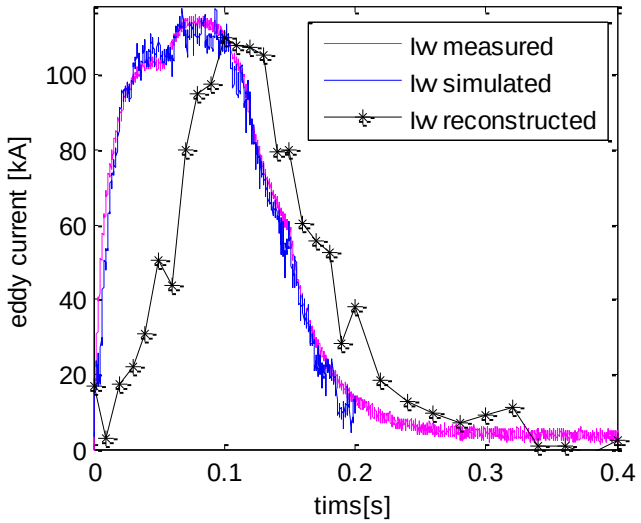

Fig. 10. Comparison of the eddy currents in the vessel and the cryostat for a vacuum discharge (shot 2068).

Next, the effect of eddy currents during the current ramp phase was estimated using the FEM model. Though the vessel structure is up-down symmetric and eddy currents will not generate Br at the midplane, it turns out eddy currents flowing in the up-down asymmetric cryostat structure may provide the required Br for the downshift. Therefore, the cryostat is included in the dynamic modeling of eddy currents and electric field generation during current ramps. In fig. 9, the effect of eddy currents in the cryostat is shown on the loop voltage. When the cryostat is included in the FEM model, the simulated voltage is in better agreement with the measured flux loop voltage. This suggests the effect of the cryostat is not trivial and its effect is larger for up-down symmetrically installed outer flux loops (the upper FL01 and the lower FL45). Without the cryostat in the model, the discrepancy is larger than 2 V for the outer FLs. However, when taking into account the eddy currents in the cryostat, the simulated voltages are in much better agreement with the measured loop voltages and the effect of cryostat on the loop voltage is pronounced for the outer loops. In addition, the eddy currents in the cryostat reproduce qualitatively the up-down asymmetry in the measured loop voltages, i.e., the FL45, which is at the lower outside, has a lower voltage than the FL01, which is at the

upper outside.

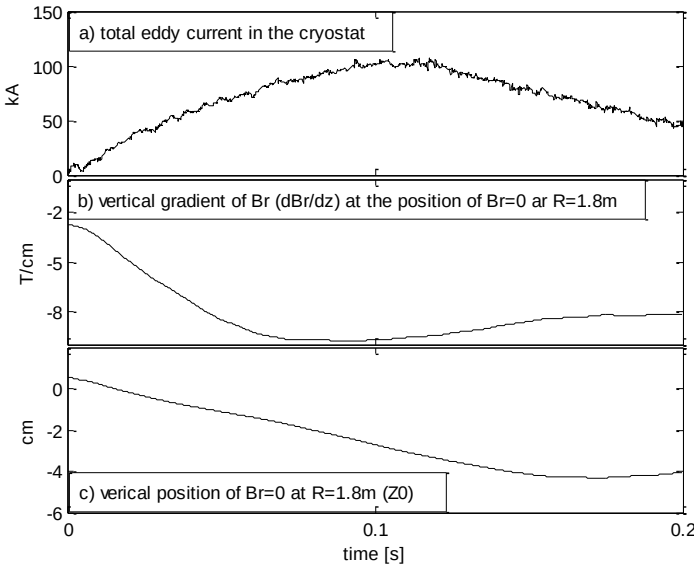

Fig. 11. The time evolution of the position where Br is zero and the local gradient of Br at Z0 (shot 2068).

In fig. 10, the simulated eddy currents are compared with the measured and the reconstructed eddy currents. The reconstruction of the eddy currents is based on the FEM model with currents in 14 segments of the vessel to be fitted using magnetic probes along the vessel surface. Although the reconstructed and measured voltages are slightly different due to the accuracy in the probe and the vessel model, the simulated and measured time evolutions of the vessel currents are in good agreement with the given PF currents.

In fig. 11, the time traces are shown of the vertical position Z0, where Br=0, and also the value of the gradient of Br at Z0. The calculated eddy currents in the cryostat are not small, as estimated from the loop voltage, and potentially it provides the Br for downshift of the plasma. According to the FEM model, the eddy currents in the cryostat generate several gauss of Br at the midplane. The location Z0, where Br is zero, is equivalent to the plasma Z position and it shifts downward further as the eddy currents increase. After t=100 ms when the eddy currents decrease as shown in Fig 10, Z0 continues downward due to the reduced (i.e. less negative) dBr/dz. The value of Z0 is dependent also on the gradient of Br. As the gradient of Br is reduced, the shift of Z0 continues with the same Br generation from eddy currents. Therefore, Z0 will be determined not only by additional Br from the up-down asymmetric source of eddy currents but also by the change of the gradient of Br. In conclusion, judging from the vacuum shot analysis with the FEM model, the downshift of the plasma is qualitatively accounted by eddy currents in the cryostat and these currents generate a few gauss of additional Br near the field-null center. However, this downshift may be easily compensated with slightly up-down asymmetric charging of either the outer PF coils or the in-vessel control coils which are available from the 2010 campaign of KSTAR.

References

[1] I. Hwang, et al., *Adv. Cry. Eng. Mat.*, vol.38, p1, 1992.
[2] A. C. England, S. W. Yoon, W. C. Kim, et al., "Tokamak Field Error Measurements with an Electron Beam in KSTAR," Fusion Eng. Des. (2010), doi:10.1016/j.fusengdes. 2010.07.021.
[3] J.A. Wesson, *Tokamaks* 2nd ed., Clarendon Press, Oxford (2004).